Geochemical Perspectives Letters

An oxygen isotope test for the origin of Archean mantle roots

M.E. Regier, A. Mišković, R.B. Ickert, D.G. Pearson, T. Stachel, R.A. Stern, M. Kopylova

Supplementary Information

The Supplementary Information includes:

- Supplementary Methods
- Tables S-1 to S-4
- Figures S-1 and S-2
- Supplementary Information References

Supplementary Methods

Mount preparation and ion probe analysis is credited to the Canadian Centre for Isotopic Microanalysis (CCIM) at the University of Alberta. Minerals were arrayed on double-sided tape, cast in 25 mm epoxy disks, and then ground and polished using diamond grits. The CCIM primary reference materials (RMs) are olivine S0013D (Mg# = 0.93) and S0103 (Mg# = 0.744). The mounts were coated with 10 nm of high-purity Au prior to scanning electron microscopy (SEM) utilising a Zeiss EVO MA15 instrument. Beam conditions were 15kV and 3 nA sample current. A further 40 nm of Au was subsequently deposited on the mount prior to SIMS analysis.

Oxygen isotopes (^{18}O, ^{16}O) were analysed using a Cameca IMS 1280 multicollector ion microprobe. A $^{133}Cs+$ primary beam was operated with an impact energy of 20 keV and beam current of 1.8 – 2.2 nA. The ~10 µm diameter probe was rastered (20 x 20 µm) for 45 s prior to acquisition, and then typically reduced to 8 x 8 µm during acquisition, forming analyzed areas ~15 µm across and ~2 µm deep. The normal incidence electron gun was utilised for charge compensation. Negative secondary ions were extracted with 10 kV into the secondary column. Conditions included a 122 µm entrance slit, a 5 x 5 mm pre-ESA (field) aperture, and 100x sample magnification at the field aperture, transmitting all regions of the sputtered area. No energy filtering was employed. The mass/charge separated oxygen ions were detected simultaneously in Faraday cups L'2 ($^{16}O^-$) and H'2 ($^{18}O^-$) at mass resolutions (m/Δm at 10 %) of 1950 and 2250, respectively. Secondary ion count rates for $^{16}O^-$ and $^{18}O^-$ were typically ~2 x 10^9 and 4 x 10^6 counts/s utilising 1010 Ω and 1011 Ω amplifier circuits, respectively. Faraday cup baselines were measured at the start of the analytical session. A single analysis took 240 s, including pre-analysis rastering, automated secondary ion tuning, and 75 s of continuous peak counting.

Instrumental mass fractionation (IMF) was monitored by repeated analysis of the primary olivine and enstatite standard (olivine S0013D $\delta^{18}O_{VSMOW}$ = +5.26 ‰; enstatite S0170 $\delta^{18}O_{VSMOW}$ = +5.64 ‰; R. Stern, unpublished laser fluorination data, University of Oregon). One analysis of the primary RM was taken after every 4 unknowns. The $^{18}O^-/^{16}O^-$ data set for each primary RM was processed collectively for its session, yielding a standard deviation ranging from = 0.07 ‰ to 0.12 ‰, following correction for systematic within-session drift of ≤0.3 ‰. IMF values for olivine were corrected for EPMA-determined Mg#s by + 0.038 ‰/Mg# unit relative to the IMF determined for S0013D olivine, determined on a separate mount (M0290) containing S0013D and S0103 olivine. Opx $\delta^{18}O$ was corrected for Mg# using laser fluorination data from 94.1 Mg# sample F866 (Lowry *et al.* 1999) and 91.2 Mg# standard enstatite S0170 (R. Stern, unpublished laser fluorination data, University of Oregon). The 95 % confidence uncertainty

estimates for $\delta^{18}O_{VSMOW}$ average ±0.21 ‰.

Supplementary Tables

Table S-1 $\delta^{18}O$ and major elements for cratonic olivine samples in this study. Major elements from Boyd and Finnerty (1980), Boyd *et al.* (1997), Canil *et al.* (1994), Carlson *et al.* (1999), Fitch *et al.* (1983), Griffin *et al.* (1993), Heaman *et al.* (1997), Heaman *et al.* (2004), Irvine *et al.* (2003), König *et al.* (2014), Kopylova and Russell, (2000), Kopylova *et al.* (1999), Kramers and Smith (1983), Kramers *et al.* (1983), Larsen *et al.* (1992), Lowry *et al.* (1999), Mather (2012), Mattey (1994), Pearson *et al.* (2004), Pearson *et al.* (1995a), Pearson *et al.* (1995b), Richardson (1986), Sand *et al.* (2009), Secher *et al.* (2009), Yudin *et al.* (2014), Viljoen (1994), Wartho and Kelley (2003), Wittig *et al.* (2010).

Sample	Reference	Craton	Lithology	$\delta^{18}O_{VSMOW}$ (‰)	2σ	olivine Mg#	ΔMg/Si
9-2	this study	Slave	Lherzolite	5.01	0.20	92.0	-0.01
39-23	this study	Slave	Lherzolite	5.04	0.20	92.8	0.13
28-15	this study	Slave	Lherzolite	5.06	0.20	91.8	-0.06
Let28	this study	Kaapvaal	Harzburgite	5.06	0.20	92.9	-0.06
F865	Mattey *et al.* 1994	Kaapvaal	Harzburgite	5.07	0.20	n.a	-0.06
JFL H1	Mattey *et al.* 1994	Kaapvaal	Harzburgite	5.07	0.20	n.a	n.a
Let29	this study	Kaapvaal	Harzburgite	5.09	0.20	92.5	-0.07
M5	this study	Kaapvaal	Lherzolite	5.11	0.20	91.9	-0.07
KV9	Mattey *et al.* 1994	Kaapvaal	Harzburgite	5.13	0.20	n.a	n.a
PHN5273	this study	Kaapvaal	Harzburgite	5.13	0.20	92.6	-0.14
22-1	this study	Slave	Lherzolite	5.14	0.20	92.3	-0.07
Let2	this study	Kaapvaal	Harzburgite	5.15	0.20	93.3	-0.02
53-10	this study	Slave	Lherzolite	5.15	0.20	92.1	0.06
JJG 147	Mattey *et al.* 1994	Kaapvaal	Harzburgite	5.15	0.20	n.a	n.a
FRB909	Mattey *et al.* 1994	Kaapvaal	Lherzolite	5.15	0.20	n.a	n.a
DDM_327	this study	Slave	Lherzolite	5.15	0.20	90.4	-0.12
Opx-rich	this study	Kaapvaal	Lherzolite	5.16	0.20	92.9	n.a
M12	this study	Kaapvaal	Lherzolite	5.16	0.20	92.2	n.a
10-12A	this study	Slave	Lherzolite	5.18	0.20	92.5	-0.02
DDM_367	this study	Slave	Lherzolite	5.18	0.20	91.4	0.01
UV47/76	Mattey *et al.* 1994	Siberia	Dunite	5.19	0.20	n.a	n.a
PHN 5275	Mattey *et al.* 1994	Kaapvaal	Lherzolite	5.19	0.20	n.a	n.a
25-4	this study	Slave	Lherzolite	5.19	0.20	91.8	-0.02
K13A3	this study	Rae	Lherzolite	5.20	0.20	92.4	-0.03
DDM_164	this study	Slave	Lherzolite	5.20	0.20	92.7	-0.13
DDM_368	this study	Slave	Lherzolite	5.21	0.20	91.7	-0.06
DDM_332	this study	Slave	Lherzolite	5.21	0.20	91.8	-0.06
LQ29	this study	Kaapvaal	Lherzolite	5.22	0.20	92.4	n.a
DDM_360	this study	Slave	Lherzolite	5.22	0.20	91.2	0.04
JFL L1	Mattey *et al.* 1994	Kaapvaal	Lherzolite	5.23	0.20	n.a	n.a
LET 38	this study	Kaapvaal	Lherzolite	5.23	0.20	93.3	-0.14
M9	this study	Kaapvaal	Lherzolite	5.23	0.20	92.0	-0.15
FRB1350	this study	Kaapvaal	Lherzolite	5.24	0.20	91.7	-0.10
G-06-06b	this study	N. Atlantic	Dunite	5.26	0.20	91.7	0.08
X07	this study	Rae	Harzburgite	5.26	0.20	92.5	-0.07
UV18-1	this study	Siberia	Dunite	5.27	0.20	92.6	n.a
M18/LQ2	this study	Kaapvaal	Dunite	5.27	0.20	92.5	n.a
126742B	this study	N. Atlantic	Harzburgite	5.27	0.20	91.4	n.a
K15A4	this study	Rae	Lherzolite	5.27	0.20	92.7	0.01
LQ1	this study	Kaapvaal	Harzburgite	5.27	0.20	93.1	0.00
K11A14	this study	Rae	Lherzolite	5.27	0.20	92.4	0.05
JPN-9	this study	Rae	Lherzolite	5.28	0.20	92.2	0.02
UV 413/89	Mattey *et al.* 1994	Siberia	Lherzolite	5.28	0.20	n.a	n.a
PHN 5267	Mattey *et al.* 1994	Kaapvaal	Lherzolite	5.28	0.20	n.a	n.a
UV18-2	this study	Siberia	Dunite	5.29	0.20	92.3	n.a
PHN 5246	Mattey *et al.* 1994	Kaapvaal	Lherzolite	5.29	0.20	n.a	n.a
UV67/76	this study	Siberia	Harzburgite	5.29	0.20	92.4	n.a
MX5023	this study	Slave	Lherzolite	5.29	0.20	92.6	-0.01
LGS 40 (MX19)	this study	Slave	Lherzolite	5.30	0.20	92.8	n.a

126739	this study	N. Atlantic	Harzburgite	5.30	0.20	90.9	n.a
G-06-07d	this study	N. Atlantic	Dunite	5.30	0.20	91.6	0.22
UV 69/76	this study	Siberia	Dunite	5.37	0.20	93.0	n.a
39670	this study	N. Atlantic	Harzburgite	5.31	0.20	91.6	n.a
K12A1	this study	Rae	Lherzolite	5.31	0.20	92.4	0.05
FRB1434	this study	Kaapvaal	Harzburgite	5.32	0.20	93.1	-0.08
K18-1	this study	Kaapvaal	Harzburgite	5.32	0.20	92.2	n.a
UV18-4	this study	Siberia	Dunite	5.33	0.20	92.3	n.a
JD1 (MX1)	this study	Slave	Lherzolite	5.33	0.20	90.1	n.a
N2B (PHA90)	this study	Rae	Lherzolite	5.33	0.20	90.8	0.06
UV4776	this study	Siberia	Dunite	5.33	0.20	92.4	n.a
F866	this study	Kaapvaal	Harzburgite	5.33	0.20	93.1	n.a
G-06-04c	this study	N. Atlantic	Lherzolite	5.34	0.20	91.3	0.11
UV 49/76	this study	Siberia	Dunite	5.30	0.20	92.9	n.a
UV18-3	this study	Siberia	Dunite	5.35	0.20	92.4	n.a
JPN-3B	this study	Rae	Lherzolite	5.35	0.20	91.9	-0.07
JP2-X2	this study	Rae	Lherzolite	5.36	0.20	92.2	-0.03
F556	Mattey *et al.* 1994	Kaapvaal	Lherzolite	5.37	0.20	n.a.	-0.26
26-11	this study	Slave	Lherzolite	5.37	0.20	92.3	-0.05
DDM_339	this study	Slave	Lherzolite	5.37	0.20	89.8	-0.06
PHN5239	this study	Kaapvaal	Lherzolite	5.37	0.20	91.7	-0.05
JP3-X1	this study	Rae	Harzburgite	5.37	0.20	92.4	0.04
DDM_366	this study	Slave	Lherzolite	5.37	0.20	91.3	n.a
JPN-4	this study	Rae	Lherzolite	5.37	0.20	91.9	0.00
LET 49	this study	Kaapvaal	Harzburgite	5.38	0.20	91.3	0.01
FRB909	this study	Kaapvaal	Lherzolite	5.40	0.20	91.3	-0.18
N1C	this study	Rae	Lherzolite	5.40	0.20	92.1	0.05
477406c	this study	N. Atlantic	Wehrlite	5.40	0.20	92.7	n.a
UV 70/76	this study	Siberia	Dunite	5.41	0.20	93.1	n.a
JPS-6B	this study	Rae	Lherzolite	5.42	0.20	91.9	0.06
K11A18	this study	Rae	Lherzolite	5.43	0.20	92.4	0.10
UV 417/89	this study	Siberia	Lherzolite	5.43	0.20	91.2	-0.01
DDM_384	this study	Slave	Lherzolite	5.46	0.20	91.7	-0.17
DDM_335	this study	Slave	Lherzolite	5.52	0.20	91.2	-0.02
DDM_444	this study	Slave	Lherzolite	5.53	0.20	91.4	-0.12
Ave $\delta^{18}O$	**5.26**						
MORB corrected	**5.47**						
2σ	**0.22**						

Table S-2 $\delta^{18}O$ and major elements for cratonic Opx samples in this study.

Sample	$\delta^{18}O$ reference	Locality	Craton	Lithology	Opx Mg#	Opx $\delta^{18}O$	2σ	ΔMg /Si
PHN 5273	Mattey *et al.* 1994	Premier	Kaapvaal	harzburgite	92.6	5.70	0.2	-0.14
FRB 1350	Mattey *et al.* 1994	Premier	Kaapvaal	lherzolite	91.7	5.84	0.2	-0.10
F865	Mattey *et al.* 1994	Finsch	Kaapvaal	harzburgite	n.a.	5.63	0.2	-0.06
F866	Lowry *et al.* 1999	Finsch	Kaapvaal	harzburgite	94.1	5.76	0.2	n.a.
JJG 147	Lowry *et al.* 1999	Finsch	Kaapvaal	harzburgite	n.a.	5.63	0.2	n.a.
PHN 5239	this study	Premier	Kaapvaal	lherzolite	92.2	5.52	0.2	-0.05
08/81	this study	Obhazhennaya	Siberian	opx-pyroxenite	92.8	5.82	0.2	n.a.
GP402	this study	Kimberley	Kaapvaal	harzburgite	94.6	5.76	0.2	n.a.
GMM2002/1	this study	Kimberley	Kaapvaal	lherzolite	93.9	5.97	0.2	n.a.
Ave $\delta^{18}O$	**5.74**							
2σ	**0.27**							

Table S-3 $\delta^{18}O$ and major elements for non-cratonic fore-arc olivine samples.

Sample	Locality	Lithology	Olivine $\delta^{18}O$	2σ	olivine Mg#
GP02/108	Horoman peridotite massif, Japan	Harzburgite	5.31	0.20	91.3
DM18-1	Dun Mountain, New Zealand	Harzburgite	5.29	0.20	90.6

Table S-4 pMELTS (Ghiorso and Hirschmann, 2002) isenthalpic AFC output for slab melt interacting with 95 wt. % Fo93 and 5 wt. % clinoen statite, and $\delta^{18}O$ mass balance modeling. Slab melt composition from Rapp *et al.* (1999), water-fluxed depleted mantle melt from (Mitchell and Grove, 2015). $\Delta^{18}O_{crystals\text{-}melt}$ from Eiler (2001). Initial oxygen fugacity set at QFM-1. *Initial slab melt $\delta^{18}O$ is an average of the lava section of an ophiolite compilation model (Ickert *et al.* 2013). **Starting $\delta^{18}O$ calculated with 3 % slab derived H2O (8 ‰) and 97 % peridotite (5.5 ‰).

T °C	Melt (g)	Melt SiO_2 (g)	Opx (g)	Opx Mg#	Garnet (g)	Garnet Mg #	Olivine (g)	Olivine Mg#	$\delta^{18}O$ melt (‰)	$\delta^{18}O$ opx (‰)	$\delta^{18}O$ olivine (‰)	$\delta^{18}O$ garnet (‰)
Slab melt interacting with 1500 ℃ harzburgite*												
1365	100	66.1	0	n.a	0	n.a.	0	n.a	8.00	n.a.	n.a.	n.a.
1401	91	66.6	11	90.9	17	82.0	0	n.a	7.75	7.25	n.a.	6.95
1430	85	64.2	27	90.9	0	n.a.	0	n.a	7.46	6.96	n.a.	n.a.
1452	79	61.3	26	93.1	0	n.a.	0	n.a	7.21	6.71	n.a.	n.a.
1466	75	57.7	24	94.2	0	n.a.	0	n.a	6.91	6.72	n.a.	n.a.
1471	72	53.7	23	94.8	0	n.a.	0	n.a	6.63	6.58	n.a.	n.a.
1468	70	49.4	21	94.8	0	n.a.	0	n.a	6.36	6.46	n.a.	n.a.
1468	71	48.0	7	94.8	0	n.a.	13	94.0	6.20	6.36	5.86	n.a.
1470	72	48.0	0	94.8	0	n.a.	19	94.0	6.12	n.a.	5.77	n.a.
1471	72	48.0	0	n.a.	0	n.a.	19	94.0	6.06	n.a.	5.71	n.a.
1474	73	48.1	0	n.a.	0	n.a.	19	94.0	6.00	n.a.	5.66	n.a.
1476	74	48.1	0	n.a.	0	n.a.	19	94.0	5.97	n.a.	5.62	n.a.
1477	74	48.1	0	n.a.	0	n.a.	19	93.0	5.94	n.a.	5.59	n.a.
1479	75	48.1	0	n.a.	0	n.a.	19	93.0	5.91	n.a.	5.56	n.a.
1480	75	48.1	0	n.a.	0	n.a.	19	93.0	5.89	n.a.	5.55	n.a.
1481	76	48.1	0	n.a.	0	n.a.	19	93.0	5.88	n.a.	5.53	n.a.
Slab melt interacting with 900 ℃ harzburgite*												
1365	100	66.1	0	n.a.	0	n.a.	0	n.a.	8.00	n.a.	n.a.	n.a.
1323	77	67.9	30	90.8	23	80.7	0	n.a.	7.86	7.36	n.a.	7.06
1271	59	64.6	47	91.9	1	82.4	0	n.a.	7.63	7.18	n.a.	6.83
1211	43	57.5	46	93.1	0	n.a.	0	n.a.	7.38	7.18	n.a.	n.a.
1140	31	45.7	38	93.7	0	n.a.	4	92.0	7.14	7.38	6.88	n.a.
1050	28	43.5	7	93.7	0	n.a.	26	93.0	6.56	6.87	6.37	n.a.
989	27	42.1	4	94.2	0	n.a.	27	93.0	6.16	6.53	5.96	n.a.
950	26	41.3	3	94.2	0	n.a.	28	93.0	6.53	6.93	6.33	n.a.
791	56	41.8	0	n.a.	0	n.a.	27	93.0	6.19	n.a.	5.99	n.a.
Fluxed harzburgitic melt interacting with 1300 ℃ harzburgite**												
1403	100	55.7	0	n.a	0.0	n.a	0.0	n.a	5.60	n.a.	n.a.	n.a.
1403	97	54.5	10	91.4	0.0	n.a	0.0	n.a	5.60	5.52	n.a.	n.a.
1403	94	53.3	10	91.4	0.0	n.a	0.0	n.a	5.60	5.56	n.a.	n.a.
1402	92	52.1	10	92.5	0.0	n.a	0.0	n.a	5.59	5.60	n.a.	n.a.
1400	89	50.7	10	92.5	0.0	n.a	0.0	n.a	5.58	5.63	n.a.	n.a.
1397	87	49.3	10	93.0	0.0	n.a	0.0	n.a	5.56	5.67	n.a.	n.a.
1395	85	47.9	9	93.0	0.0	n.a	0.0	n.a	5.54	5.70	n.a.	n.a.
1391	84	47.1	6	93.0	0.0	n.a	3	93.0	5.54	5.73	5.23	n.a.
1389	83	47.0	1	93.0	0.0	n.a	7	93.0	5.56	5.75	5.25	n.a.

Supplementary Figures

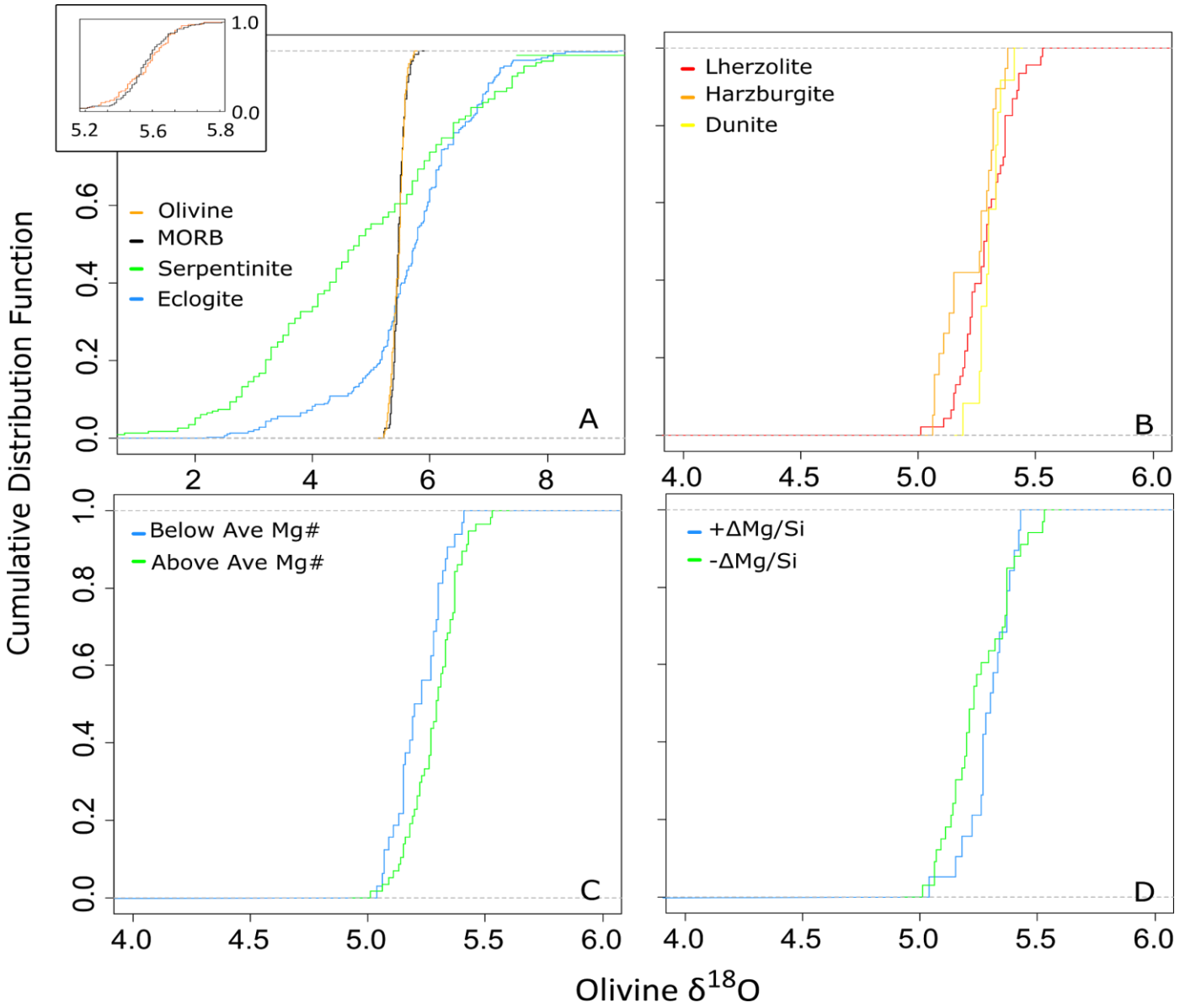

Figure S-1 **(a)** Cumulative distribution plots of various mantle rocks. MORB and olivine have statistically identical oxygen isotopes (K-S bootstrap test: D = 0.09, p = 0.86). Variances of MORB and cratonic olivines are statistically equal (F test: F111,73= 0.8486, p-value =0.4314). This can be seen in the inset. **(b)** Lherzolitic, low-Ca harzburgitic, and dunitic peridotites have statistically identical oxygen isotopes. (Dunite-harzburgite K-S bootstrap test: D = 0.42, p = 0.14. Dunite - lherzolite K-S bootstrap test: D = 0.31, p = 0.33. Harzburgite-lherzolite K-S bootstrap test: D = 0.31, p = 0.15) **(c)** Below average Mg# olivines and above average Mg# olivines have statistically identical oxygen isotopes (K-S bootstrap test: D = 0.27, p-value = 0.1). Non-statistically significant systematic offset may be due to error in Mg# ion probe matrix correction. **(d)** Si-enriched whole rock lithologies (-ΔMg/Si) and Si-depleted whole rock lithologies (+ΔMg/Si) have statistically identical oxygen isotopes (K-S bootstrap test: D = 0.37, p-value = 0.08). Whole rock serpentinized oceanic lithospheric mantle data from Agrinier *et al.* (1988), 1995, Alt *et al.* (2007), Barnes *et al.* (2009), Boschi *et al.* (2008), Cocker *et al.* (1982), Früh-Green *et al.* (2001). MORB glass data from Cooper *et al.* (2004, 2009), Eiler *et al.* (2000). Eclogite data from Appleyard (2000), Barth *et al.* (2001), Beard *et al.* (1996), Deines *et al.* (1991), Garlick *et al.* (1971), Jacob *et al.* (1994), Malkovets *et al.* (2003), Neal *et al.* (1990), Ongley *et al.* (1987), Schmickler *et al.* (2004).

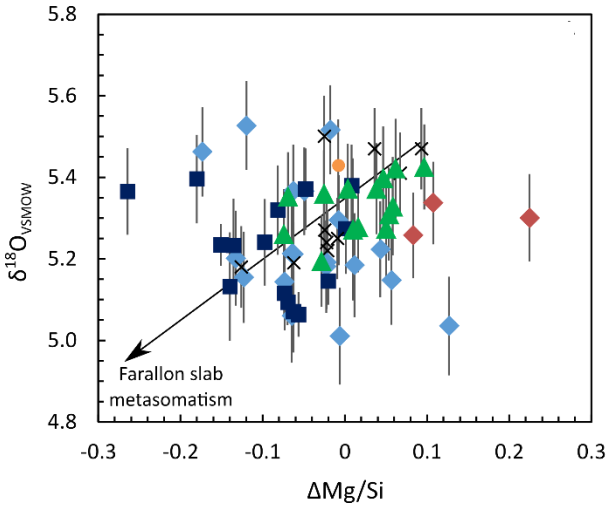

Figure S-2 Oxygen isotope compositions for olivines from subcratonic and noncratonic peridotites (this study and Mattey *et al.* 1994) compared with bulk rock Si enrichment (ΔMg/Si). Error bars are 2σ. No correlations between Si enrichment (negative ΔMg/Si) and $\delta^{18}O$ exist in subcratonic samples, but one is visible for The Thumb xenoliths ($R^2 = 0.52$). See legend in Figure 3c.

Supplementary Information References

Agrinier, P., Hékinian, R., Bideau, D., Javoy, M. (1995) O and H stable isotope compositions of oceanic crust and upper mantle rocks exposed in the Hess Deep near the Galapagos Triple Junction. *Earth and Planetary Science Letters* 136, 183–196.

Agrinier, P., Javoy, M., Girardeau, J. (1988) Hydrothermal activity in a peculiar oceanic ridge: Oxygen and hydrogen isotope evidence in the Xigaze ophiolite (Tibet, China). *Chemical Geology* 71, 313–335.

Alt, J.C., Shanks, W.C., Bach, W., Paulick, H., Garrido, C.J., Beaudoin, G. (2007) Hydrothermal alteration and microbial sulfate reduction in peridotite and gabbro exposed by detachment faulting at the Mid-Atlantic Ridge, 15° 20′ N (ODP Leg 209): A sulfur and oxygen isotope study. *Geochemistry, Geophysics, Geosystems* 8.

Appleyard, C.M. (2000) The geochemistry of a suite of eclogite xenoliths from the Rietfontein Kimberlite, South Africa. PhD dissertation, University of Cape Town.

Barnes, J.D., Paulick, H., Sharp, Z.D., Bach, W., Beaudoin, G. (2009) Stable isotope (δ18O, δD, δ37Cl) evidence for multiple fluid histories in mid-Atlantic abyssal peridotites (ODP Leg 209). *Lithos* 110, 83–94.

Barth, M.G., Rudnick, R.L., Horn, I., McDonough, W.F., Spicuzza, M.J., Valley, J.W., Haggerty, S.E. (2001) Geochemistry of xenolithic eclogites from West Africa, part I: A link between low MgO eclogites and archean crust formation. *Geochimica et Cosmochimica Acta*. 65, 1499–1527.

Beard, B.L., Fraracci, K.N., Clayton, R.A., Mayeda, T.K., Snyder, G.A., Sobolev, N.V., Taylor, L.A. (1996) Petrography and geochemistry of eclogites from the Mir kimberlite, Yakutia, Russia. *Contributions to Mineralogy and Petrology* 125, 293–310.

Boschi, C., Dini, A., Früh-Green, G.L., Kelley, D.S. (2008) Isotopic and element exchange during serpentinization and metasomatism at the Atlantis Massif (MAR 30°N): Insights from B and Sr isotope data. *Geochimica et Cosmochimica Acta* 72, 1801–1823.

Boyd, F.R., Finnerty, A.A. (1980) Conditions of origin of natural diamonds of peridotite affinity. *Journal of Geophysical Research* 85, 6911–6918.

Boyd, F.R., Pokhilenko, N.P., Pearson, D.G., Mertzman, S.A., Sobolev, N.V., Finger, L.W. (1997) Composition of the Siberian cratonic mantle: evidence from Udachnaya peridotite xenoliths. *Contributions to Mineralogy and Petrology* 128, 228–246.

Canil, D., O'Neill, H.S.C., Pearson, D.G., Rudnick, R.L., McDonough, W.F., Carswell, D.A. (1994) Ferric iron in peridotites and mantle oxidation states. *Earth and Planetary Science Letters* 123, 205–220.

Carlson, R.W., Pearson, D.G., Boyd, F.R., Shirey, S.B., Irvine, G., Menzies, A.H., Gurney, J.J., Others (1999) Re--Os systematics of lithospheric peridotites: implications for lithosphere formation and preservation. *Proceedings of the 7th International Kimberlite Conference*, 99–108.

Chiba, H., Chacko, T., Clayton, R.N., Goldsmith, J.R. (1989) Oxygen isotope fractionations involving diopside, forsterite, magnetite, and calcite: Application to geothermometry. *Geochimica et Cosmochimica Acta* 53, 2985–2995.

Cocker, J.D., Griffin, B.J., Muehlenbachs, K. (1982) Oxygen and carbon isotope evidence for seawater-hydrothermal alteration of the Macquarie Island ophiolite. *Earth and Planetary Science Letters* 61, 112–122.

Cooper, K.M., Eiler, J.M., Asimow, P.D., Langmuir, C.H. (2004) Oxygen isotope evidence for the origin of enriched mantle beneath the mid-Atlantic ridge. *Earth and Planetary Science Letters* 220, 297–316.

Cooper, K.M., Eiler, J.M., Sims, K.W.W., Langmuir, C.H. (2009) Distribution of recycled crust within the upper mantle: Insights from the oxygen isotope composition of MORB from the Australian-Antarctic Discordance. *Geochemistry, Geophysics, Geosystems* 10, Q12004.

Deines, P., Harris, J.W., Robinson, D.N., Gurney, J.J., Shee, S.R. (1991) Carbon and oxygen isotope variations in diamond and graphite eclogites from Orapa, Botswana, and the nitrogen content of their diamonds. *Geochimica et Cosmochimica Acta* 55, 515–524.

Eiler, J.M. (2001) Oxygen Isotope Variations of Basaltic Lavas and Upper Mantle Rocks. *Reviews in Mineralogy and Geochemistry* 43, 319–364.

Eiler, J.M., Schiano, P., Kitchen, N., Stolper, E.M. (2000) Oxygen-isotope evidence for recycled crust in the sources of mid-ocean-ridge basalts. *Nature* 403, 530–534.

Fitch, F.J., Miller, J.A. (1983) K-Ar age of the east peripheral kimberlite at De Beers Mine, Kimberley, RSA. *Geological magazine* 120, 505–512.

Früh-Green, G.L., Scambelluri, M., Vallis, F. (2001) O–H isotope ratios of high pressure ultramafic rocks: implications for fluid sources and mobility in the subducted

hydrous mantle. *Contributions to Mineralogy and Petrology* 141, 145–159.

Garlick, G.D., Macgregor, I.D., Vogel, D.E. (1971) Oxygen isotope ratios in eclogites from kimberlites. *Science* 172, 1025–1027.

Griffin, W.L., Sobolev, N.V., Ryan, C.G., Pokhilenko, N.P., Win, T.T., Yefimova, E.S. (1993) Trace elements in garnets and chromites: Diamond formation in the Siberian lithosphere. *Lithos* 29, 235–256.

Heaman, L.M., Kjarsgaard, B., Creaser, R.A., Cookenboo, H.O., Kretschmar, U. (1997) Multiple episodes of kimberlite magmatism in the Slave Province, North America. *Lithoprobe Workshop Report*, 14–17.

Heaman, L.M., Kjarsgaard, B.A., Creaser, R.A. (2004) The temporal evolution of North American kimberlites. *Lithos* 76, 377–397.

Ickert, R.B., Stachel, T., Stern, R.A., Harris, J.W. (2013) Diamond from recycled crustal carbon documented by coupled δ18O–δ13C measurements of diamonds and their inclusions. *Earth and Planetary Science Letters* 364, 85–97.

Irvine, G.J., Pearson, D.G., Kjarsgaard, B.A., Carlson, R.W., Kopylova, M.G., Dreibus, G. (2003) A Re–Os isotope and PGE study of kimberlite-derived peridotite xenoliths from Somerset Island and a comparison to the Slave and Kaapvaal cratons. *Lithos* 71, 461–488.

Jacob, D., Jagoutz, E., Lowry, D., Mattey, D., Kudrjavtseva, G. (1994) Diamondiferous eclogites from Siberia: Remnants of Archean oceanic crust. *Geochimica et Cosmochimica Acta* 58, 5191–5207.

König, S., Lorand, J.-P., Luguet, A., Graham Pearson, D. (2014) A non-primitive origin of near-chondritic S–Se–Te ratios in mantle peridotites; implications for the Earth's late accretionary history. *Earth and Planetary Science Letters* 385, 110–121.

Kopylova, M.G., Russell, J.K. (2000) Chemical stratification of cratonic lithosphere: constraints from the Northern Slave craton, Canada. *Earth and Planetary Science Letters* 181, 71–87.

Kopylova, M.G., Russell, J.K., Cookenboo, H. (1999) Petrology of Peridotite and Pyroxenite Xenoliths from the Jericho Kimberlite: Implications for the Thermal State of the Mantle beneath the Slave Craton, Northern Canada. *Journal of Petrology* 79–104.

Kramers, J.D., Smith, C.B. (1983) A feasibility study of U- Pb and Pb- Pb dating of kimberlites using groundmass mineral fractions and whole-rock samples. *Chemical Geology* 41, 23–38.

Kramers, J.D., Roddick, J.C.M., Dawson, J.B. (1983) Trace element and isotope studies on veined, metasomatic and "MARID" xenoliths from Bultfontein, South Africa. *Earth and Planetary Science Letters* 65, 90–106.

Larsen, L.M., Rex, D.C. (1992) A review of the 2500 Ma span of alkaline-ultramafic, potassic and carbonatitic magmatism in West Greenland. *Lithos* 28, 367–402.

Lowry, D., Mattey, D.P., Harris, J.W. (1999) Oxygen isotope composition of syngenetic inclusions in diamond from the Finsch Mine, RSA. *Geochimica et Cosmochimica Acta* 63, 1825–1836.

Malkovets, V. Taylor, L., Griffin, W., O'Reilly, S., Pokhilenko, N., Verichev, Ev., Golovin, N., Litasov, K., Valley, J., Spicuzza, M., (2003) Eclogites from the Grib kimberlite pipe, Arkhangelsk, Russia. *8th International Kimberlite Conference Extended Abstracts* p 222.

Mather, K.A. (2012) A xenolith-based lithospheric transect of the Slave Craton, N.W.T., Canada. Doctoral dissertation, Durham University.

Mattey, D., Lowry, D., Macpherson, C. (1994) Oxygen isotope composition of mantle peridotite. *Earth and Planetary Science Letters* 128, 231–241.

Muehlenbachs, K., Kushiro, I. (1974) Oxygen isotope exchange and equilibrium of silicates with CO2 or O2. Carnegie Instution of Washington Yearbook 71, 232–236.

Mitchell, A.L., Grove, T.L. (2015) Melting the hydrous, subarc mantle: the origin of primitive andesites. *Contributions to Mineralogy and Petrology* 170, 13.

Neal, C.R., Taylor, L.A., Davidson, J.P., Holden, P., Halliday, A.N., Nixon, P.H., Paces, J.B., Clayton, R.N., Mayeda, T.K. (1990) Eclogites with oceanic crustal and mantle signatures from the Bellsbank kimberlite, South Africa, part 2: Sr, Nd, and O isotope geochemistry. *Earth and Planetary Science Letters* 99, 362–379.

Ongley, J.S., Basu, A.R., Kurtis Kyser, T. (1987) Oxygen isotopes in coexisting garnets, clinopyroxenes and phlogopites of Roberts Victor eclogites: implications for petrogenesis and mantle metasomatism. *Earth and Planetary Science Letters* 83, 80–84.

Pearson, D.G., Irvine, G.J., Ionov, D.A., Boyd, F.R., Dreibus, G.E. (2004) Re-Os isotope systematics and platinum group element fractionation during mantle melt extraction: A study of massif and xenolith peridotite suites. *Chemical Geology* 208, 29–59.

Pearson, D.G., Carlson, R.W., Shirey, S.B., Boyd, F.R., Nixon, P.H. (1995a) Stabilisation of Archaean lithospheric mantle: A ReOs isotope study of peridotite xenoliths from the Kaapvaal craton. *Earth and Planetary Science Letters* 134, 341–357.

Pearson, D.G., Shirey, S.B., Carlson, R.W., Boyd, F.R., Pokhilenko, N.P., Shimizu, N. (1995b) ReOs, SmNd, and RbSr isotope evidence for thick Archaean lithospheric mantle beneath the Siberian craton modified by multistage metasomatism. *Geochimica et Cosmochimica Acta* 59, 959–977.

Rapp, R.P., Shimizu, N., Norman, Applegate, G.S. (1999) Reaction between slab-derived melts and peridotite in the mantle wedge: experimental constraints at 3.8 GPa. *Chemical Geology* 160, 335–356.

Richardson, S.H. (1986) Latter-day origin of diamonds of eclogitic paragenesis. *Nature* 322, 623.

Rosenbaum, J.M., Walker, D., Kyser, T.K. (1994) Oxygen isotope fractionation in the mantle. *Geochimica et Cosmochimica Acta* 58, 4767–4777.

Sand, K.K., Waight, T.E., Pearson, D.G., Nielsen, T.F.D., Makovicky, E., Hutchison, M.T. (2009) The lithospheric mantle below southern West Greenland: A geothermobarometric approach to diamond potential and mantle stratigraphy. *Lithos* 112, 1155–1166.

Schmickler, B., Jacob, D.E., Foley, S.F. (2004) Eclogite xenoliths from the Kuruman kimberlites, South Africa: geochemical fingerprinting of deep subduction and cumulate processes. *Lithos* 75, 173–207.

Secher, K., Heaman, L.M., Nielsen, T.F.D., Jensen, S.M., Schjøth, F., Creaser, R.A. (2009) Timing of kimberlite, carbonatite, and ultramafic lamprophyre emplacement in the alkaline province located 64°–67° N in southern West Greenland. *Lithos* 112, 400–406.

Viljoen, K.S. (1994) The petrology and geochemistry of a suite of mantle-derived eclogite xenoliths from the Kaalvallei kimberlite, South Africa. Doctoral dissertation, University of the Witwatersrand.

Wartho, J.-A., Kelley, S.P. (2003) 40Ar/39Ar ages in mantle xenolith phlogopites: determining the ages of multiple lithospheric mantle events and diatreme ascent rates in southern Africa and Malaita, Solomon Islands. *Geological Society, London, Special Publications* 220, 231–248.

Wenner, D.B., Taylor, H.P. (1971) Temperatures of serpentinization of ultramafic rocks based on O18/O16 fractionation between coexisting serpentine and magnetite. *Contributions to Mineralogy and Petrology* 32, 165–185.

Wittig, N., Webb, M., Pearson, D.G., Dale, C.W., Ottley, C.J., Hutchison, M., Jensen, S.M., Luguet, A. (2010) Formation of the North Atlantic Craton: Timing and mechanisms constrained from Re–Os isotope and PGE data of peridotite xenoliths from S.W. Greenland. *Chemical Geology* 276, 166–187.

Yudin, D.S., Tomilenko, A.A., Travin, A.V., Agashev, A.M., Pokhilenko, N.P., Orihashi, Y. (2014) The age of Udachnaya-East kimberlite: U/Pb and 40 Ar/39 Ar data. *Doklady Earth Sciences* 455, 288–290.